

# Degeneracy of velocity strain-rate tensor statistics in random isotropic incompressible flows

A. V. Kopyev\*

*P.N. Lebedev Physical Institute of the Russian Academy of Sciences,  
53 Leninskiy Prospekt, 119991, Moscow, Russia*



(Received 2 August 2017; published 13 February 2018)

The article considers the strain-rate tensor distribution in various isotropically distributed incompressible flows. By means of a fortunate choice of variables, a strong degeneracy in the probability distribution of strain-rate tensor characteristics is found in numerical simulations of isotropic turbulence. This allows us to reduce the probability density function (PDF) of the strain-rate tensor to a function of one variable. Also it appears that for those particular parameters that reflect the ratio of different eigenvalues of the strain tensor ( $s$  and  $\beta$  parameters), the shapes of their probability distributions are universal and do not depend on the specific shape of distribution. Furthermore, it is also shown analytically that for all time-reversible statistical isotropic flows the probability distribution of  $s$  is uniform, which generalizes previous numerical calculations.

DOI: [10.1103/PhysRevFluids.3.024603](https://doi.org/10.1103/PhysRevFluids.3.024603)

## I. INTRODUCTION

The velocity field in a turbulent flow is known to be stochastic. Its statistical properties have attracted the attention of researchers in physics, mechanics, and mathematics for more than a century, but the problem is still far from being solved. The velocity gradients play a significant role in different turbulent processes. In particular, they play an important role in a theoretical consideration [1] that gives physical interpretation of the known multifractal model in the isotropic turbulence. They are also responsible for the passive scalar transport [2]. Statistical properties of the velocity gradients were calculated in many direct numerical simulations (DNSs) and were measured in a wide range of experiments (see the overview [3] and the references therein). There are also many phenomenological theoretical models for these quantities (see the overview [4] and the references therein).

### A. Short overview of the previous results

This article studies the case of incompressible isotropic turbulent flow. Statistical properties of the strain-rate tensor, which is known to be a symmetrical part of the full velocity gradient tensor are considered:

$$S_{ij} = \frac{1}{2} \left( \frac{\partial u_i}{\partial x_j} + \frac{\partial u_j}{\partial x_i} \right). \quad (1)$$

In most of the research concerning the problem (e.g., Refs. [5–17]), the statistical properties of the strain-rate tensor are considered in terms of its rotation invariants; these are the combinations of the tensor components that do not depend on the rotation of the coordinate system. For instance, the

---

\*kopyev@lpi.ru

eigenvalues of the tensor [13–15] or traces of its powers [12–16] can play the role of such invariants:

$$P_S = -\text{Tr}(S) \equiv 0, \quad (2)$$

$$Q_S = -\frac{1}{2}\text{Tr}(S^2), \quad (3)$$

$$R_S = -\frac{1}{3}\text{Tr}(S^3), \quad (4)$$

where  $P_S$  is equal to zero due to incompressibility of the flow. The traces of greater strain-rate tensor powers are the explicit functions of  $Q_S$  and  $R_S$  because there are only two independent rotation invariants for this tensor [4]. Consideration of two independent rotation invariants is sufficient to describe the statistics of isotropic flow [5,18].

There are other rotation invariants called normalized eigenvalues ( $s$  and  $\beta$ ); their single PDFs do not give the full statistic information of the strain but are useful in considering fluid particle deformation tendencies. Each of these values gives the unique strain-rate tensor eigenvalue ratio but says nothing about the absolute values of the eigenvalues. Since these invariants were introduced and analyzed in Refs. [6,7], their statistics have been investigated in many articles (e.g., Refs. [8–11,13,17]). The measured single PDFs of the normalized eigenvalues show little dependence on the turbulent flow characteristics; i.e., they almost repeat themselves for different flows from paper to paper (compare corresponding figures in Refs. [6–8,10,11,17]).

Concerning theoretical investigations, most results can only be deduced for Gaussian distributed quantities. This makes Gaussian distributions topical in turbulence research in spite of the well-known distinctive features of the turbulence statistics such as irreversibility and intermittency.

We can divide these studies into two parts. The first part uses phenomenological reasons to model some nonlinear processes in dynamical equations by Gaussian processes to close the statistical equations [4,19]. The second part of the studies, which this article follows to some extent, was pioneered in Ref. [20] and concerns various statistical properties in normally distributed isotropic velocity field to compare them with the ones numerically or experimentally obtained from isotropic turbulent velocity field. Such approach does not use dynamical equations, and thus the properties obtained in the case of the normally distributed velocity field can be considered kinematic [21].

## B. Present article results

The mathematical basis of the article and notation for different PDFs is placed in Appendix A, where we derive different relations between PDFs of strain-rate tensor components and their different rotation invariants.

We start Sec. II by defining rotation invariants  $\xi_+$  and  $\xi_-$ . Their PDF is plotted for the DNS data extracted from the Johns Hopkins University (JHU) turbulence database (JHTDB) [22,23]. This PDF in the most part of its domain turns out to have linear parallel contour levels; this allows us to reduce it to a one-dimensional function. In Sec. III, it is shown analytically that this symmetry also takes place in statistically isotropic time-reversible flows.

## II. STRAIN-RATE TENSOR DISTRIBUTION SYMMETRY IN FORCED ISOTROPIC TURBULENCE

Let us introduce the following non-negative rotation invariant combinations:

$$\begin{aligned} \xi_+ &= (-Q_S)^{3/2} + \frac{3\sqrt{3}}{2}R_S, \\ \xi_- &= (-Q_S)^{3/2} - \frac{3\sqrt{3}}{2}R_S. \end{aligned} \quad (5)$$

We plot the PDF of  $\xi_+$  and  $\xi_-$  based on the data from JHU turbulence database [24]. Figure 1 shows that the PDF of  $\xi_+$  and  $\xi_-$  depends almost purely on the linear combination of invariants  $\xi_+$

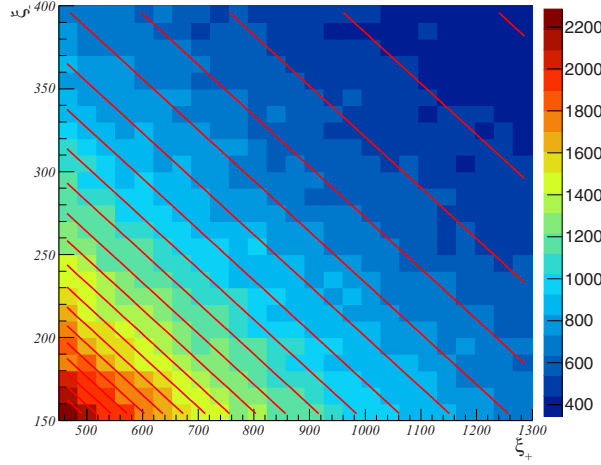


FIG. 1. The histogram of invariants  $\xi_+$  and  $\xi_-$  in the JHTDB distribution case (i.e., obtained from JHU database). The red lines show the symmetry. Note that the horizontal scale differs from the vertical scale, and the levels of the function are skewed to the horizontal axis.

and  $\xi_-$ :

$$\xi_a = \frac{1+a}{2}\xi_+ + \frac{1-a}{2}\xi_-, \quad (6)$$

where  $a \sim -0.6 \div -0.5$  is a fixed constant parameter. Hence, the PDF of invariants  $\xi_+$  and  $\xi_-$  turns degenerate in the JHTDB distribution case (we designated the distribution simulated in the database as “JHTDB distribution” by analogy with Gaussian distribution). The invariant  $\xi_a$  introduced in (6) will be useful in our further consideration. It can be also expressed in terms of invariants  $Q_S$  and  $R_S$ :

$$\xi_a = (-Q_S)^{3/2} + \frac{3\sqrt{3}a}{2}R_S. \quad (7)$$

#### A. Estimation of symmetry parameter

We now introduce the normalized eigenvalues  $s$  and  $\beta$  mentioned in the introduction [6,7]:

$$s = \frac{-3\sqrt{6}\lambda_1\lambda_2\lambda_3}{(\lambda_1^2 + \lambda_2^2 + \lambda_3^2)^{3/2}} = \frac{3\sqrt{3}R_S}{2(-Q_S)^{3/2}}, \quad (8)$$

$$\beta = \frac{\sqrt{6}\lambda_2}{\sqrt{\lambda_1^2 + \lambda_2^2 + \lambda_3^2}}. \quad (9)$$

Here  $\lambda_1$ ,  $\lambda_2$ , and  $\lambda_3$  are the eigenvalues of the strain-rate tensor in decreasing order. Both  $s$  and  $\beta$  can change in the interval  $[-1; 1]$ . It turns out that the symmetry found above produces exact relations for  $s$  and  $\beta$  PDFs; they depend on the symmetry parameter  $a$  only. In addition, this allows us to calculate the symmetry parameter precisely.

Using the PDF of  $\xi_+$  and  $\xi_-$ , the discovered symmetry can be expressed as follows:

$$f_{\xi_+\xi_-}(x_+, x_-) = f\left(\frac{1+a}{2}x_+ + \frac{1-a}{2}x_-\right), \quad (10)$$

where  $x_+$  and  $x_-$  are arguments of the PDF that are responsible for  $\xi_+$  and  $\xi_-$ , respectively, and  $f$  is a function of one variable. By calculation of the Jacobian of the transformation from  $\xi_+$  and  $\xi_-$  to

$Q_S$  and  $R_S$ , the following relation between their PDFs can be calculated:

$$f_{Q_S R_S}(q, r) = \frac{9\sqrt{3}}{2}(-q)^{1/2} \cdot f_{\xi_+ \xi_-} \left( (-q)^{3/2} + \frac{3\sqrt{3}}{2}r, (-q)^{3/2} - \frac{3\sqrt{3}}{2}r \right). \quad (11)$$

Here  $q$  and  $r$  are the arguments of the PDF corresponding to  $Q_S$  and  $R_S$ , respectively. From (10) and (11), one can obtain

$$f_{Q_S R_S}(q, r) = \frac{9\sqrt{3}}{2}(-q)^{1/2} f \left( (-q)^{3/2} + \frac{3\sqrt{3}}{2}ar \right). \quad (12)$$

From the latter relation for the  $Q_S$  and  $R_S$  PDF, one can obtain the relation for the single PDF of the normalized eigenvalue  $s$  (see Appendix A3 for details):

$$f_s = 6 \int_0^{+\infty} f(t^3(1+as))t^5 dt. \quad (13)$$

By changing  $t$  to  $t\sqrt[3]{1+as}$ , one can see that the considered PDF does not depend on specific shape of the function  $f$ :

$$f_s \propto \frac{1}{(1+as)^2}. \quad (14)$$

Normalization of  $f_s$  finally results in

$$f_s = \frac{(1-a^2)}{2(1+as)^2}. \quad (15)$$

Analogously, universality of the PDF of  $\beta$  can be found:

$$f_\beta = \frac{3}{4}(1-\beta^2) \frac{(1-a^2)}{(1+\frac{a}{2}\beta(3-\beta^2))^2}. \quad (16)$$

To find  $a$ , relation (15) can be rewritten in a more convenient way:

$$\sqrt{\frac{1}{f_s}} = \sqrt{\frac{2}{1-a^2}}(1+as). \quad (17)$$

This means that  $f_s^{-1/2}$  depends linearly on its argument. It is illustratively confirmed by Fig. 2. This dependence can be approximated by means of the least-squares fitting that leads to the following value of  $a$  for JHTDB distribution:

$$a \simeq -0.53. \quad (18)$$

The fitting line with its analytical expression placed over the numerical results is also depicted in Fig. 2.

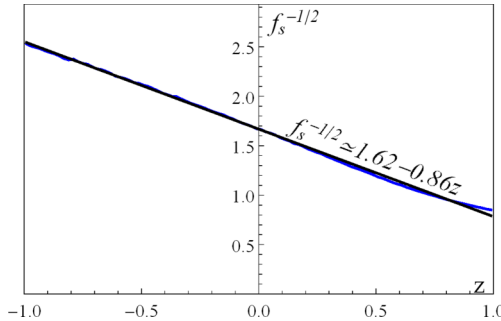


FIG. 2. Dependence of  $f_s^{-1/2}$  on  $s$  in the JHTDB distribution case and linear fitting (17) of  $f_s^{-1/2}$  on  $s$  in the JHTDB distribution case with its analytical expression.

### B. Full strain-rate tensor statistic degeneracy

In Appendix A 2, we deduce an important relation between the strain-rate tensor  $S_{ij}$  distribution (a function of five variables) and the  $Q_S$  and  $R_S$  PDF (depending on two variables), where summation over repeated indices is assumed:

$$f_S\{\sigma\} = \frac{1}{2\pi^2} f_{Q_S R_S} \left( -\frac{1}{2} \sigma_{ij} \sigma_{ji}, -\frac{1}{3} \sigma_{ij} \sigma_{jk} \sigma_{ki} \right). \quad (19)$$

Here the subscript  $S$  is used to indicate the strain-rate tensor PDF; we also introduce the multivariable  $\{\sigma\} = (\sigma_{11}, \sigma_{22}, \sigma_{12}, \sigma_{13}, \sigma_{23})$  for an argument of the PDF,  $\sigma_{ij}$  corresponding to  $S_{ij}$ . Together with (12), this equation means that the full strain-rate tensor statistics can also be written in terms of the function  $f$  of one variable.

### III. STRAIN-RATE TENSOR STATISTICS IN THE CASE OF ISOTROPIC TIME-REVERSIBLE DISTRIBUTIONS

This section proves analytically that for statistically isotropic time-reversible flows the symmetry (10) also takes place with parameter  $a$  equal to zero.

One can conclude that the statistic irreversibility appears due to the skewness of its PDF as a result of the prevalence of direct processes over inverse ones. On the contrary, reversible statistics must contain equal number of direct and inverse processes on the average. This is reflected in the fact that the reversible distribution of strain-rate tensor  $S_{ij}$  depends on invariant  $Q_S$  only [5]. Because of this, in Appendix A 2 we prove a nontrivial fact: For reversible distributions, the PDF of invariants  $Q_S$  and  $R_S$  also depends on argument  $q$  only,

$$f_{Q_S R_S}(q, r) = f_{\text{rev}}(q), \quad (20)$$

where  $f_{\text{rev}}$  is a function of one variable. Using the expression reciprocal to (11), one can obtain for the PDF of invariants  $\xi_+$  and  $\xi_-$ :

$$f_{\xi_+ \xi_-}(x_+, x_-) = \frac{2^{4/3} f_{\text{rev}} \left( -\frac{1}{2^{2/3}} (x_+ + x_-)^{2/3} \right)}{9\sqrt{3} (x_+ + x_-)^{1/3}}. \quad (21)$$

The latter relation shows that the symmetry (10) with parameter  $a$  equal to zero takes place in the case of arbitrary time-reversible distribution. Thus, by substituting  $a = 0$  in (15) and (16), the universal time-reversible shapes of  $s$  and  $\beta$  PDFs can be deduced:

$$f_s = \frac{1}{2}, \quad (22)$$

$$f_\beta = \frac{3}{4} (1 - \beta^2). \quad (23)$$

The calculated shapes of  $f_s$  and  $f_\beta$  are in absolute agreement with the previous numerical calculations for the Gaussian distribution [8], which is known to be a specific case of time-reversible distribution (red dot-dashed and blue dashed curves in Fig. 3 coincide with dotted curves in Figs. 1(a) and 1(b) in Ref. [8] respectively). That is, this section generalizes the numerical results [8] for any arbitrary time-reversible case.

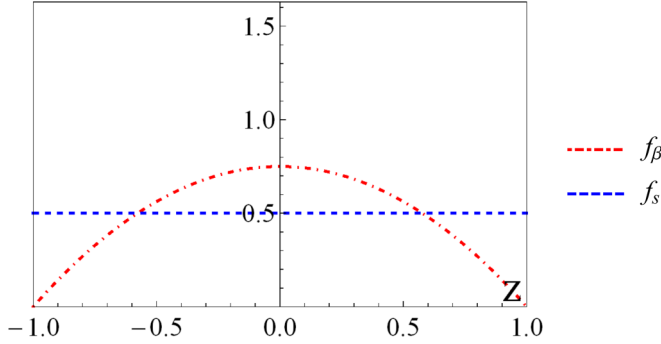


FIG. 3. PDFs (22) and (23) of parameters  $s$  and  $\beta$  in the case of time-reversible distribution.

### A. Gaussian distribution case

The relations deduced in Appendix A make it possible to calculate analytically the PDFs of different strain-rate tensor invariants in random isotropic incompressible velocity field with Gaussian statistics. The analysis of this case is placed in Appendix B.

### B. Possible influence of large-scale stochastic energy sources on the zero region of turbulent statistic

It can be seen in Fig. 4 that the distribution is not skewed in the small region of invariants  $\xi_+$  and  $\xi_-$  near the origin. There is less than 1% of the distribution in this region and, thus, it naturally could be designated as the “zero region.” Therefore, parameter  $a$  is not constant and becomes zero in the zero region, which means time reversibility of the JHTDB statistic in this region. The presence of some Gaussian (or other time-reversible) noises, which are the result of the large-scale energy production, is a possible natural mechanism of such a phenomenon. For instance, in the JHU turbulence database, this noise production is achieved by keeping constant the total energy in modes with the small wave-number magnitude. Physically it is equivalent to adding some stochastic force with time-reversible statistics (to keep the full energy constant).

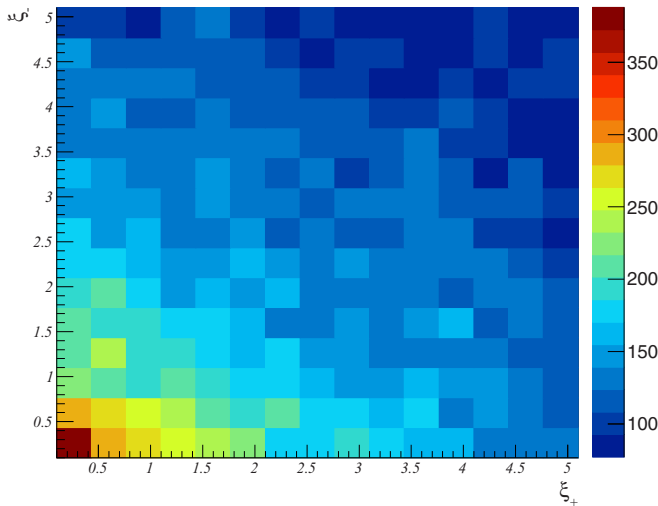


FIG. 4. The histogram of invariants  $\xi_+$  and  $\xi_-$  in the zero region in the JHTDB distribution.

#### IV. CONCLUSION

In this article, strain-rate tensor statistics in incompressible isotropic stochastic flows is considered. Rotation invariants  $\xi_+$  and  $\xi_-$  are introduced in (5). Their distribution  $f_{\xi_+\xi_-}$  turns out to have the symmetry (10) both for isotropic turbulence simulated in the JHU database, with  $a = -0.53$  (see Sec. II), and for time-reversible distributions, with  $a = 0$  (see Sec. III). The consequences of this symmetry are the following: First, it leads to universality of the normalized eigenvalues ( $s$  and  $\beta$ ) distributions; second, it means degeneracy of the complete distribution of strain-rate tensor components.

High precision of the presented degeneracy gives us some hope that it provides the true asymptotic behavior for the strain-rate statistics in isotropic turbulence. However, this result, whether it is general or only approximate, is a challenge for further theoretical studies.

#### ACKNOWLEDGMENTS

I am much obliged to my scientific supervisor Prof. K. P. Zybin for his interest in my work and fruitful discussions. I am thankful to Prof. V. A. Sabelnikov for discussions and to S. A. Velichko and I. O. Polyakov for help with extracting and processing the data. The work was supported by the Russian Science Foundation (RSF) Grant No. 17-11-01271.

#### APPENDIX A: PDFS OF DIFFERENT STRAIN-RATE TENSOR INVARIANTS AND RELATIONS BETWEEN THEM

In this Appendix, we provide the analytical approach for PDFs analysis by deducing different relations and integral transformations between PDFs of strain-rate tensor components and its different rotation invariants in cases of isotropy and incompressibility.

##### 1. PDF of strain-rate tensor eigenvalues

In fact, the eigenvalues depend nonlinearly on strain-rate tensor components. Now we find the transformation from the strain-rate tensor distribution to the strain-rate tensor eigenvalues PDF. Let

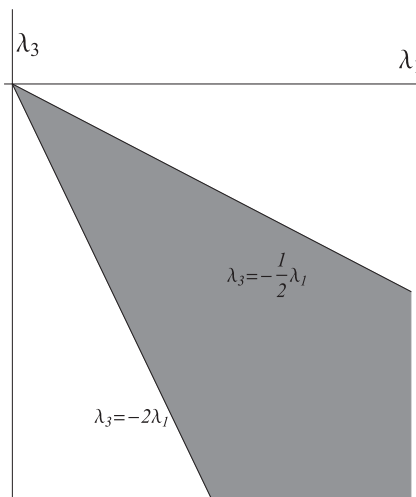


FIG. 5. The domain of the maximum strain-rate tensor eigenvalue  $\lambda_1$  and the minimum strain-rate tensor eigenvalue  $\lambda_3$  (grayscale).

us introduce the strain-rate tensor PDF of five variables:

$$f_S(\sigma_{11}, \sigma_{22}, \sigma_{12}, \sigma_{13}, \sigma_{23}) = f_S\{\sigma\}. \quad (\text{A1})$$

Subscript  $S$  means that the function is the strain-rate tensor PDF; we also introduce multivariable  $\{\sigma\} = (\sigma_{11}, \sigma_{22}, \sigma_{12}, \sigma_{13}, \sigma_{23})$  for convenience. The subscript of PDF ( $S$ ) denotes the physical quantity it corresponds to. Notations for variables ( $\sigma$ ) differ from the subscript according to mathematical notation system [25,26] chosen in this article.

As was mentioned in the introduction, the strain-rate tensor PDF in the case of the statistical isotropy includes five variables in the form of two orientation-invariant combinations. Such combinations are, for instance, either invariants  $Q_S(S_{11}, S_{22}, S_{12}, S_{13}, S_{23}) = Q_S\{S\} = -\frac{1}{2}S_{ij}S_{ji}$  and  $R_S\{S\} = -\frac{1}{3}S_{ij}S_{jk}S_{ki}$  or eigenvalues  $\lambda_1\{S\}$  and  $\lambda_3\{S\}$  (summation over repeated indices is assumed):

$$f_S\{\sigma\} = f_S^{Q_S R_S} \left( -\frac{1}{2}\sigma_{ij}\sigma_{ji}, -\frac{1}{3}\sigma_{ij}\sigma_{jk}\sigma_{ki} \right) \quad (\text{A2})$$

$$= f_S^{\lambda_1 \lambda_3}(\lambda_1\{\sigma\}, \lambda_3\{\sigma\}). \quad (\text{A3})$$

In (A2) and (A3), superscripts denote the invariant combinations of strain-rate tensor components. Let us turn from the tensor components coordinate system to the one including  $\lambda_1$  and  $\lambda_3$ :

$$\begin{aligned} & f_S\{\sigma\} \underbrace{d\sigma_{11}d\sigma_{22}d\sigma_{12}d\sigma_{13}d\sigma_{23}}_{d^5\{\sigma\}} \\ &= f_S^{\lambda_1 \lambda_3}(\lambda_1\{\sigma\}, \lambda_3\{\sigma\})d^5\{\sigma\} \\ &= f_S^{\lambda_1 \lambda_3}(x, y) \underbrace{\left\| \frac{\partial(S_{11}, S_{22}, S_{12}, S_{13}, S_{23})}{\partial(\lambda_1, \lambda_3, P_1, P_2, P_3)} \right\|}_{J(x, y, p_1, p_2, p_3)} \bigg|_{\substack{\lambda_1 = x, \lambda_3 = y \\ P_1 = p_1, P_2 = p_2 \\ P_3 = p_3}} dx dy dp_1 dp_2 dp_3 \\ &= f_S^{\lambda_1 \lambda_3}(x, y) |J(x, y, p_1, p_2, p_3)| dx dy dp_1 dp_2 dp_3, \end{aligned} \quad (\text{A4})$$

where  $P_1 = P_1\{S\}$ ,  $P_2 = P_2\{S\}$ , and  $P_3 = P_3\{S\}$  are any strain-rate tensor components combinations independent of  $\lambda_1$  and  $\lambda_3$  and  $J(x, y, p_1, p_2, p_3)$  is the Jacobian of the transformation from the strain-rate tensor components to the coordinate system including  $\lambda_1$  and  $\lambda_3$ . Thus, we can introduce and express the PDF of  $\lambda_1$  and  $\lambda_3$  as follows:

$$f_{\lambda_1 \lambda_3}(x, y) = f_S^{\lambda_1 \lambda_3}(x, y) \iiint |J(x, y, p_1, p_2, p_3)| dp_1 dp_2 dp_3. \quad (\text{A5})$$

It is common knowledge that under coordinate transformation a PDF is multiplied by the Jacobian. That is why the PDF of the eigenvalues  $f_{\lambda_1 \lambda_3}(x, y)$  is not equal to the function  $f_S^{\lambda_1 \lambda_3}(x, y)$  and demands its own notation.

It has been shown (see Ref. [27] and references therein) that in the case of SO(3) symmetry, the triple integral in (A5) can be written in the form

$$\iiint |J(x, y, p_1, p_2, p_3)| dp_1 dp_2 dp_3 = A|(x - y)(2x + y)(x + 2y)|, \quad (\text{A6})$$

where  $A$  is a constant factor, which is shown in Appendix B to be equal to  $2\pi^2$ . Hence, finally, by substitution (A6) in (A5) we get for the  $f_{\lambda_1 \lambda_3}(x, y)$  domain (i.e., inside the sector  $\{x \geq -x - y; y \leq -x - y\}$  depicted in Fig. 5):

$$f_{\lambda_1 \lambda_3}(x, y) = A|(x - y)(2x + y)(x + 2y)| f_S^{\lambda_1 \lambda_3}(x, y) \quad (\text{A7})$$

$$= 2\pi^2 |(x - y)(2x + y)(x + 2y)| f_S^{\lambda_1 \lambda_3}(x, y). \quad (\text{A8})$$

## 2. PDF of strain-rate tensor invariants $Q_S$ and $R_S$

The domain  $D_{Q_S R_S}$  of invariants  $Q_S$  and  $R_S$  (3) is shown in Fig. 6. It is bounded by the curves  $R_S = \pm \frac{2}{3\sqrt{3}}(-Q_S)^{3/2}$  in the lower half plane [12,16]. We introduce the PDF of invariants  $Q_S$  and  $R_S$ , which we note  $f_{Q_S R_S}(q, r)$ . Relation between the strain-rate tensor eigenvalues PDF  $f_{\lambda_1 \lambda_3}(x, y)$  and the PDF of  $Q_S$  and  $R_S$  invariants can be deduced:

$$f_{\lambda_1 \lambda_3}(x, y) = |(x - y)(2x + y)(x + 2y)| f_{Q_S R_S}(-x^2 - xy + y^2, xy(x + y)), \quad (\text{A9})$$

where  $|(x - y)(2x + y)(x + 2y)|$  is the Jacobian of the transformation from  $(Q_S; R_S)$  plane to  $(\lambda_1; \lambda_3)$  plane. Comparing (A7) and (A9) with use of (A2) and (A3), we find a simple relation between  $f_{Q_S R_S}(q, r)$  and  $f_S^{Q_S R_S}(q, r)$ :

$$f_{Q_S R_S}(q, r) = 2\pi^2 f_S^{Q_S R_S}(q, r). \quad (\text{A10})$$

This relation means that in the time-reversible distribution case considered in Sec. III,  $f_{Q_S R_S}(q, r)$  depends on variable  $q$  only. This fact is not trivial:  $f_{\lambda_1 \lambda_3}(x, y)$  in this case does not depend on the combination  $x^2 + xy + y^2$  only, because of the nontrivial Jacobian presence in an analogous relation (A7).

From (A10) and (A2) one can also derive a very important expression reciprocal to (A10); it determines the strain-rate tensor distribution of five variables via the  $Q_S$  and  $R_S$  PDF of two variables:

$$f_S\{\sigma\} = \frac{1}{2\pi^2} f_{Q_S R_S} \left( -\frac{1}{2} \sigma_{ij} \sigma_{ji}, -\frac{1}{3} \sigma_{ij} \sigma_{jk} \sigma_{ki} \right). \quad (\text{A11})$$

## 3. PDF of parameter $s$

Making use of the definition of  $s$  (8), it is possible to get the  $s$  PDF from  $f_{Q_S R_S}$ . It can be done by the integral transformation:

$$f_s = \int_{-\infty}^0 dq \int_{-\frac{2}{3\sqrt{3}}(-q)^{3/2}}^{\frac{2}{3\sqrt{3}}(-q)^{3/2}} f_{Q_S R_S}(q, r) \delta \left( s - \frac{3\sqrt{3}r}{2(-q)^{3/2}} \right) dr. \quad (\text{A12})$$

Here  $\delta(s - g(q, r))$  is the Dirac  $\delta$  function [28] on the surface  $g(q, r)$ ; the integration domain  $D_{Q_S R_S}$  is shown in Fig. 6. The calculation (A12) can be reduced to the following expression:

$$f_s = \frac{4}{3\sqrt{3}} \int_0^{+\infty} f_{Q_S R_S} \left( -t^2, t^3 \frac{2s}{3\sqrt{3}} \right) t^4 dt, \quad (\text{A13})$$

where  $s \in [-1; 1]$ . It is used in the article to obtain (13).

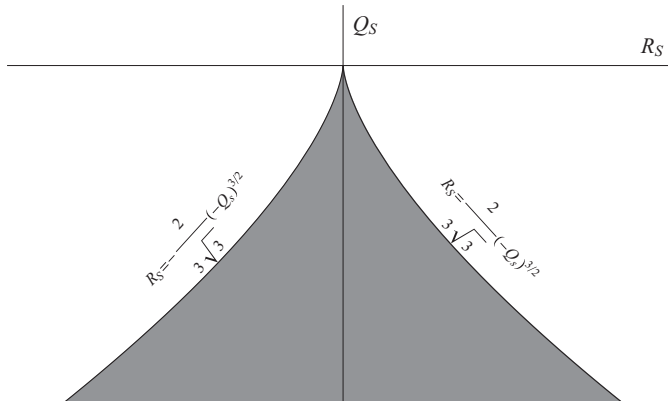


FIG. 6.  $D_{Q_S R_S}$ : the domain of  $Q_S$  and  $R_S$  invariants (grayscale).

#### 4. PDF of parameter $\beta$

Now we proceed to deducing analogous integral transformations for  $\beta$ . To do it, we use the explicit relations between parameters  $s$  and  $\beta$  given in Ref. [6]:

$$\begin{cases} \beta = 2 \sin\left(\frac{1}{3} \arcsin s\right) \\ s = \beta(3 - \beta^2)/2 \end{cases}. \quad (\text{A14})$$

Determining the Jacobian of transformation (A14) and using (A13), we can find

$$f_\beta = \frac{2}{\sqrt{3}}(1 - \beta^2) \int_0^{+\infty} f_{Q_s R_s} \left( -t^2, t^3 \frac{\beta(3 - \beta^2)}{3\sqrt{3}} \right) t^4 dt, \quad (\text{A15})$$

where  $\beta \in [-1; 1]$ .

#### APPENDIX B: CALCULATIONS FOR GAUSSIAN DISTRIBUTION CASE

In this Appendix, we will consider the random isotropic incompressible velocity field with Gaussian statistics (the Gaussian distribution case).

In Ref. [21], it was shown that from the isotropic Gaussian distribution of the flow velocity follows the Gaussian distribution of the velocity gradient tensor components and particularly of the strain-rate tensor components. In the incompressible case, the form of the strain-rate tensor components PDF is the following:

$$f_s\{\sigma\} = \frac{\sqrt{3}}{2} \left( \frac{5}{2\pi \langle \omega^2 \rangle} \right)^{5/2} \exp \left[ -\frac{5}{2 \langle \omega^2 \rangle} (\sigma_{11}^2 + \sigma_{11}\sigma_{22} + \sigma_{22}^2 + \sigma_{12}^2 + \sigma_{23}^2 + \sigma_{13}^2) \right], \quad (\text{B1})$$

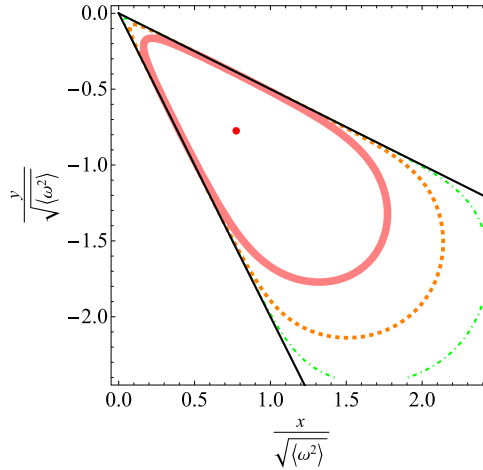


FIG. 7. Joint PDF of the maximum and the minimum strain-rate tensor eigenvalues in the Gaussian distribution case. The axes are made dimensionless through dividing by  $\langle \omega^2 \rangle$  in the corresponding degrees: This makes the PDF contour shape universal. The difference between every two neighbor contour levels is one decade. The exponents of the decade level are the following: 0 for the red point (the maximum of PDF),  $-1$  for the pink thickest contour,  $-2$  for the orange dashed one, and  $-3$  for the green dot-dashed one.

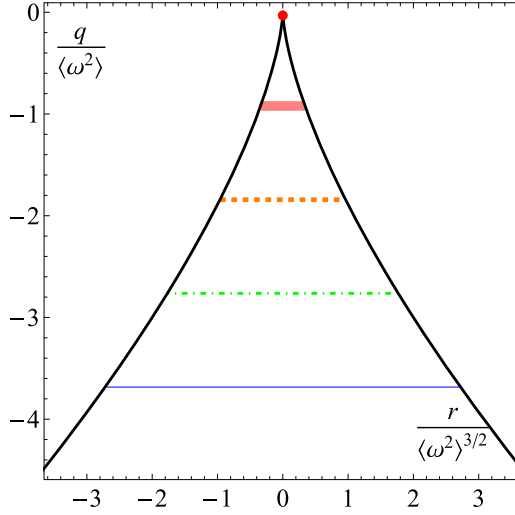


FIG. 8. Joint PDF of invariants  $Q_S$  and  $R_S$  in the Gaussian distribution case. The axes labels are made dimensionless by means of dividing by  $\langle \omega^2 \rangle$  in corresponding powers: This makes the PDF contour shape universal. The difference between every two neighbor contour levels is one decade. The exponents of the decade level are the following: 0 for the red point (the maximum of PDF),  $-1$  for the pink thickest contour,  $-2$  for the orange dashed one,  $-3$  for the green dot-dashed one, and  $-4$  for the blue thick one.

where  $\langle \omega^2 \rangle$  is the expectancy of squared vorticity of the flow. Using, this we can find from (A7) the shape of the eigenvalues PDF, which is depicted by a contour graphic in Fig. 7:

$$f_{\lambda_1 \lambda_3}(x, y) = \frac{\sqrt{3}A}{2} \left( \frac{5}{2\pi \langle \omega^2 \rangle} \right)^{5/2} |(x-y)(2x+y)(x+2y)| \exp \left[ -\frac{5}{2\langle \omega^2 \rangle} (x^2 + xy + y^2) \right]. \quad (\text{B2})$$

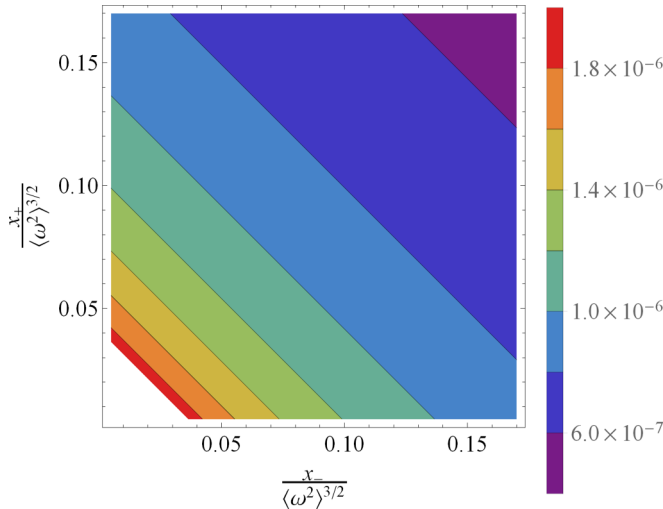


FIG. 9. Joint PDF (B5) of invariants  $\xi_+$  and  $\xi_-$  in the case of Gaussian distribution with  $\langle \omega^2 \rangle = 125$ . The axes labels are made dimensionless by means of dividing the function arguments by  $\langle \omega^2 \rangle^{3/2}$ . The function levels are shown in the legend. The white region corresponds to the function singularity. The levels shape shows  $f_{\xi_+ \xi_-}$  dependence on the linear combination of its arguments (i.e.,  $\frac{x_+ + x_-}{2}$ ) only, which means that for the Gaussian distribution the parameter of symmetry (10) is equal to  $a = 0$ .

By using normalization of  $f_{\lambda_1 \lambda_3}$  we now can find the parameter  $A$  without direct calculation of integral (A6):

$$A = 2\pi^2. \quad (\text{B3})$$

Then from (A10) we find the joint PDF of  $Q_S$  and  $R_S$  invariants, which is also depicted by a contour graphic in Fig. 8:

$$f_{Q_S R_S}(q, r) = \sqrt{\frac{3}{\pi}} \left( \frac{5}{2\langle \omega^2 \rangle} \right)^{5/2} \exp \left[ \frac{5}{2\langle \omega^2 \rangle} q \right]. \quad (\text{B4})$$

Also, the PDF of  $\xi_+$  and  $\xi_-$  can be easily found from the inverse to (11) relation:

$$f_{\xi_+ \xi_-}(x_+, x_-) = \frac{8}{9\sqrt{\pi}(x_+ + x_-)^{1/3}} \left( \frac{5}{2^{5/3}\langle \omega^2 \rangle} \right)^{5/2} \exp \left[ -\frac{5}{2^{5/3}\langle \omega^2 \rangle} (x_+ + x_-)^{2/3} \right]. \quad (\text{B5})$$

It can be seen that  $f_{\xi_+ \xi_-}$  satisfies symmetry (21) deduced in Sec. III for the arbitrary time-reversible case. Also it has a singularity at the origin. The contours of the function for  $\langle \omega^2 \rangle = 125$  are shown in Fig. 9.

- 
- [1] K. P. Zybin and V. A. Sirota, Model of stretching vortex filaments and foundations of the statistical theory of turbulence, *Phys. Usp.* **58**, 556 (2015).
  - [2] A. S. Il'yn, V. A. Sirota, and K. P. Zybin, Passive scalar transport by a non-Gaussian turbulent flow in the batchelor regime, *Phys. Rev. E* **96**, 013117 (2017).
  - [3] J. M. Wallace, Twenty years of experimental and direct numerical simulation access to the velocity gradient tensor: What have we learned about turbulence? *Phys. Fluids* **21**, 021301 (2009).
  - [4] C. Meneveau, Lagrangian dynamics and models of the velocity gradient tensor in turbulent flows, *Annu. Rev. Fluid Mech.* **43**, 219 (2010).
  - [5] A. S. Il'yn and K. P. Zybin, Material deformation tensor in time-reversal symmetry breaking turbulence, *Phys. Lett. A* **379**, 650 (2015).
  - [6] R. M. Kerr, Histograms of Helicity and Strain in Numerical Turbulence, *Phys. Rev. Lett.* **59**, 783 (1987).
  - [7] W. T. Ashurst, A. Kerstein, R. M. Kerr, and C. H. Gibson, Alignment of vorticity and scalar gradient with strain rate in simulated Navier-Stokes turbulence, *Phys. Fluids* **30**, 2343 (1987).
  - [8] T. S. Lund and M. M. Rogers, An improved measure of strain state probability in turbulent flows, *Phys. Fluids* **6**, 1838 (1994).
  - [9] A. Tsinober, E. Kit, and T. Dracos, Experimental investigation of the field of velocity gradients in turbulent flows, *J. Fluid Mech.* **242**, 169 (1992).
  - [10] A. Pumir, E. Bodenschatz, and H. Xu, Tetrahedron deformation and alignment of perceived vorticity and strain in a turbulent flow, *Phys. Fluids* **25**, 035101 (2013).
  - [11] O. R. H. Buxton, S. Laizet, and B. Ganapathisubramani, The effects of resolution and noise on kinematic features of fine-scale turbulence, *Exp. Fluids* **51**, 1417 (2011).
  - [12] A. Ooi, J. Martin, J. Soria, and M. S. Chong, A study of the evolution and characteristics of the invariants of the velocity-gradient tensor in isotropic turbulence, *J. Fluid. Mech.* **381**, 141 (1999).
  - [13] R. Gomes-Fernandes, B. Ganapathisubramani, and J. C. Vassilicos, Evolution of the velocity-gradient tensor in a spatially developing turbulent flow, *J. Fluid. Mech.* **756**, 252 (2014).
  - [14] B. Luthi, A. Tsinober, and W. Kinzelbach, Lagrangian measurement of vorticity dynamics in turbulent flow, *J. Fluid. Mech.* **528**, 87 (2005).
  - [15] G. Gulitski, M. Kholmyansky, W. Kinzelbach, B. Luthi, A. Thinober, and S. Yorish, Velocity and temperature derivatives in high-Reynolds-number turbulent flows in the atmospheric surface layer, part 1: Facilities, methods and some general results, *J. Fluid. Mech.* **589**, 57 (2007).

- [16] J. Soria, R. Sondergaard, B. Cantwell, M. Chong, and A. Perry, A study of the fine-scale motions of incompressible time-developing mixing layers, *Phys. Fluids* **6**, 871 (1994).
- [17] Z.-S. She, E. Jackson, and S. A. Orszag, Structure and dynamics of homogeneous turbulence: Models and simulations, *Proc. R. Soc. London, Ser. A* **434**, 101 (1991).
- [18] H. Weyl, *The Classical Groups. Their Invariants and Representations* (Princeton University Press, Princeton, NJ, 1939).
- [19] M. Wilczek and C. Meneveau, Pressure Hessian and viscous contributions to velocity gradient statistics based on Gaussian random fields, *J. Fluid Mech.* **756**, 191 (2014).
- [20] R. H. Kraichnan and R. Panda, Depression of nonlinearity in decaying isotropic turbulence, *Phys. Fluids* **31**, 2395 (1988).
- [21] L. Shtilman, M. Spector, and A. Tsinober, On some kinematic versus dynamic properties of homogeneous turbulence, *J. Fluid Mech.* **247**, 65 (1993).
- [22] Y. Li, E. Perlman, M. Wan, Y. Yang, R. Burns, C. Meneveau, R. Burns, S. Chen, A. Szalay, and G. Eyink, A public turbulence database cluster and applications to study Lagrangian evolution of velocity increments in turbulence, *J. Turbulence* **9**, N31 (2008).
- [23] E. Perlman, R. Burns, Y. Li, and C. Meneveau, Data exploration of turbulence simulations using a database cluster, *Supercomputing* **SC07** (2007).
- [24] Since the divergence-free condition in the simulation is enforced based on the spectral representation of the derivatives, we put  $S_{33}$  to be equal to  $-S_{11} - S_{22}$  and considered this traceless counterpart of the strain-rate tensor.
- [25] A. N. Shiryaev, *Probability-1* (Springer, Berlin, 2016).
- [26] P. Billingsley, *Probability and Measure* (John Wiley & Sons, New York, 1986).
- [27] M. L. Mehta, *Random Matrices* (Elsevier/Academic Press, San Diego, CA, 2004).
- [28] I. M. Gel'fand and G. E. Shilov, *Properties and Operations*, Vol. 1 of *Generalized Functions* (Academic Press, San Diego, CA, 1964).